Dalton Transactions

ROYAL SOCIETY OF CHEMISTRY

COMMUNICATION

View Article Online
View Journal | View Issue

Cite this: *Dalton Trans.*, 2021, **50**, 5428

Received 20th February 2021,
Accepted 1st April 2021

DOI: 10.1039/d1dt00569c

rsc.li/dalton

1D Mn(III) coordination polymers exhibiting chiral symmetry breaking and weak ferromagnetism†

Aoi Hara,[a] Sotaro Kusumoto,[a] Yoshihiro Sekine,[a,b] Jack Harrowfield,[c] Yang Kim,[a] Shinya Hayami *[a,d] and Masaaki Nakamura*[a]

Mn(III) complexes with achiral ligands, (*E*)-*N*-(2-((2-aminobenzylidene)amino)-2-methylpropyl)-5-X-2-hydroxybenzamide (HL^X, X = H, Cl, Br, and I), crystallise as chiral conglomerates containing amide oxygen-bridged one-dimensional coordination polymers that exhibit weak ferromagnetism. The bulk products exhibit symmetry breaking in that they do not contain equal amounts of enantiomers, though which is the dominant species depends on the substituent X.

The dominance of one enantiomeric form is a well-known feature of biological molecules such as amino acids, sugars and their derivatives, and its origins are intriguing.[1] Chiral materials have attracted wide interest because of their uses, for example, in asymmetric catalysis,[2] enantioselective separation or optical resolution,[3] nonlinear optics,[4] and chiral sensing.[5] Since the time of Pasteur's discovery[6] in 1848 of the crystallisation of optically active hemihedral crystals from a solution of racemic sodium ammonium tartrate and his recognition that the crystals could be dissolved to give an optically active solution, optical (chiral) resolution by direct crystallisation[7] has attracted much attention. Chiral molecules most commonly crystallise as racemic compounds, where both enantiomers are present in equal amounts in the one crystal, and sometimes as pseudoracemates where the quantities are not equal but a small fraction (5–10%) crystallise as conglomerates[8] where the crystals are chiral and contain only one or the other enantiomer. Chiral crystals can be also formed from achiral constituents, quartz being the oldest known example, though many others are known.[9] Simple, formally achiral inorganic materials such as $NaBrO_3$ and $NaClO_3$ form chiral crystals[10] and this has been analysed in Viedma's model of chiral symmetry breaking.[11] Only a few examples of chiral symmetry breaking during crystallisation from an achiral solvent have been reported,[12] providing a stimulus to search for further examples and their potential for applications.

Coordination polymers showing both magnetism and optical activity can be used for the development of multifunctional materials such as multiferroics[13] or magneto-chiral dichromics (MChD).[14] We previously reported a chiral 1D coordination polymer, $[MnL^H]_n$ (L^H = 2-hydroxy-*N*-[2-[[(2-aminophenyl)methylene]amino]-2-methylpropyl]-benzamide), crystallising in space group $P2_12_12_1$ and showing weak ferromagnetism (H_c = 3.0 kOe, $T_N \approx 7$ K) due to spin canting.[15] We herein report the structures and magnetic properties of 1D Mn(III) coordination polymers formed from the achiral ligands, (*E*)-*N*-(2-((2-aminobenzylidene)amino)-2-methylpropyl)-5-**X**-2-hydroxybenzamide (HL^X, **X** = H, Cl, Br, I), as well as the crystallisation of each complex resulting in conglomerates but with unequal amounts of the enantiomers.

Complexes, $[MnL^X]_n$ (**X** = H (**1**), Cl (**2**), Br (**3**), and I (**4**)) (Fig. 1a), were prepared as previously described.[15] The elemen-

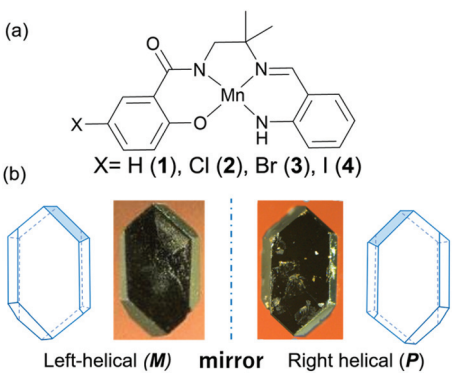

Fig. 1 (a) Structure of the complex unit; (b) crystal shapes of **4**.

[a]*Department of Chemistry, Graduate School of Science and Technology, Kumamoto University, 2-39-1 Kurokami, Chuo-ku, Kumamoto 860-8555, Japan. E-mail: hayami@kumamoto-u.ac.jp*
[b]*Priority Organization for Innovation and Excellence, Kumamoto University, 2-39-1 Kurokami, Chuo-ku, Kumamoto 860-8555, Japan*
[c]*ISIS, Université de Strasbourg, 8 allée Gaspard Monge, 67083 Strasbourg, France*
[d]*Institute of Industrial Nanomaterials (IINa), Kumamoto University, 2-39-1 Kurokami, Chuo-ku, Kumamoto 860-8555, Japan*

†Electronic supplementary information (ESI) available. CCDC 2060011–2060016. For ESI and crystallographic data in CIF or other electronic format see DOI: 10.1039/d1dt00569c

tal analyses and FT-IR spectra indicated triply deprotonated ligands and the absence of counter anions. All formed crystals with the space group $P2_12_12_1$, indicating that spontaneous resolution had occurred. Crystallisation of complex **4** from methanol gave large crystals of readily identified mirror image forms, and more than 60 were successfully separated under a microscope for further experiments (Fig. 1b). Complexes **1**, **2**, and **3**, however, formed thin, plate-like crystals that could not be visually distinguished (Fig. S1†). Structure determinations on over 30 crystals of each complex established that the complexes **1** to **4** crystallise invariably as conglomerates, not racemic compounds.

X-ray structure determinations showed that the Mn(III) coordination geometry in all was that of a distorted square pyramid, involving the N_3O donor set of each ligand in the four positions of the basal plane and an amide oxygen (bond lengths 2.081–2.117 Å) from a ligand on an adjacent Mn(III), thus generating a helical 1D coordination polymer. Each of the mirror image crystals of complex **4** contains either right-handed- (***P***) or left-handed (***M***) helical polymer units running parallel to the *a*-axis of the unit cell (Fig. 2), although crystals of ***M*** structure were rare in comparison to those with ***P*** (*vide infra*). The conformation of the central five-membered chelate ring, C8–N1–Mn–N2–C9, is λ in the ***P*** polymer and δ in the ***M*** (Fig. 2 and Fig. S2–3†) in all four structures.

The helix pitches (7.855 to 9.501 Å), the shortest intrachain Mn···Mn distances (5.772 to 6.075 Å) and $\angle$Mn–O_{amide}–C7 (134.65 to 165.41°) as well as the intermetallic distances (10.452–12.729 Å) between neighboring Mn(III) ions of the polymer depend on the halogen substituent on the phenolate ring of the ligand (Fig. S4 and S5†) possibly due to differences in dispersion interactions. Examination of the Hirshfeld surfaces for the complexes provides no substantial evidence for halogen bonding interactions (Fig. S6†). Only in the case of X = Cl does there appear to be a weak Cl···C3(aromatic) interaction. Otherwise, the closest atoms to the halogens in all cases are H-atoms, indicating that there is no expansion of the halogen's valence shell. The PXRD patterns of compounds **1** to **4** were identical with those simulated from the structure determinations (Fig. S7†).

The solid-state circular dichroism (CD) spectra of enantiomerically pure samples of complexes **1** to **4** were measured in KBr pellets (Fig. S8†), and reflected the helix handedness, *i.e.* the samples with the ***P*** structure showed positive Cotton effects in the first d–d transition region and those with ***M***, negative effects. The CD spectra of coordination compounds are usually considered in terms of the symmetric metal ion chromophore being perturbed by several additive effects leading to symmetry reduction.[16] While the Mn(III)N_3O_2 chromophore is inherently symmetric, it is perturbed both by its incorporation into the helical polymer and by the chiral conformation of the central five-membered chelate ring of the ligand, thus becoming dissymmetric (Fig. 2 and Fig. S2†). The measurable circular dichroism in the solid state (Fig. S8†) is due to the loss of any symmetry at the metal ion site and the presence of a single enantiomer in the crystals. When enantiomerically pure crystals of **1** to **4** were dissolved in methanol, no circular dichroism was detected (Fig. S9†), consistent with the lability of Mn(III) causing dissociation of the polymer units and inversion of the five-membered chelate ring in solution being extremely rapid.

Although enantiomorphic crystals must have identical solubility in achiral solvents, so that where racemic, configurationally stable, chiral molecules form chiral crystals the conglomerate deposited from a solution of the racemate should ultimately contain equal amounts of each enantiomer, in practice, where yields are commonly <100%, this is often found not to be the case.[17] It is even more frequently observed not to be so when chiral crystals are formed, as here, from achiral components or from chiral compounds which undergo rapid racemisation in solution.[11,18,19]

As the sense of vortices created by stirring may influence solute chirality,[20] each synthesis was repeated a few times with either clockwise or anticlockwise stirring and solid-state CD spectra then measured on the whole products (Fig. 3a–d). In all cases, one or the other enantiomer predominated, *i.e.* for complex **1** the crystals were mainly the ***M*** structure but for compounds **2**, **3** and **4**, mainly the ***P***, with no systematic dependence on the sense of stirring. For compound **3**, there are also some cases with no predominant crystallisation of ***M*** or ***P*** (Fig. 3e). Similar results were also obtained without stirring (Fig. S10†). Although numerous causes of symmetry breaking in spontaneous resolution have been postulated,[19–22] a consensus of opinion does not exist. Analysis[23] of the 'Meyerhoffer double solubility rule' relating to differences in racemisation rates in the presence and absence of a crystallised enantiomer has provided an understanding of 'Viedma ripening'[11] such as can lead to the isolation of but a single enantiomorph with simple materials like $NaClO_3$. Chiral symmetry breaking in fluids such as liquid crystals has been reported,[24] and rationalised in terms of aggregate formation. It has also been reported that selective chiral symmetry breaking can be the result of Parity-violating energy differences (PVED) which cause any two enantiomers, most markedly those containing heavy elements,

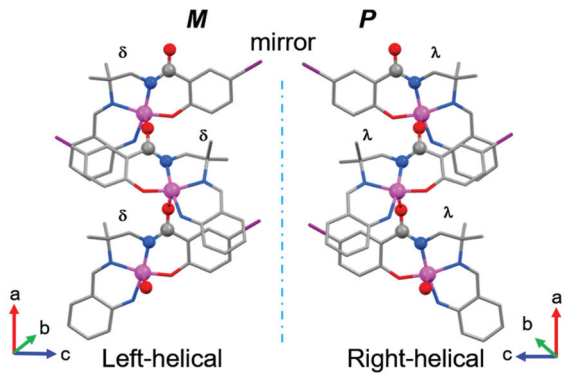

Fig. 2 Mirror image forms of the helical coordination polymers of **4** viewed down the *b*-axis. Hydrogen atoms are omitted for clarity.

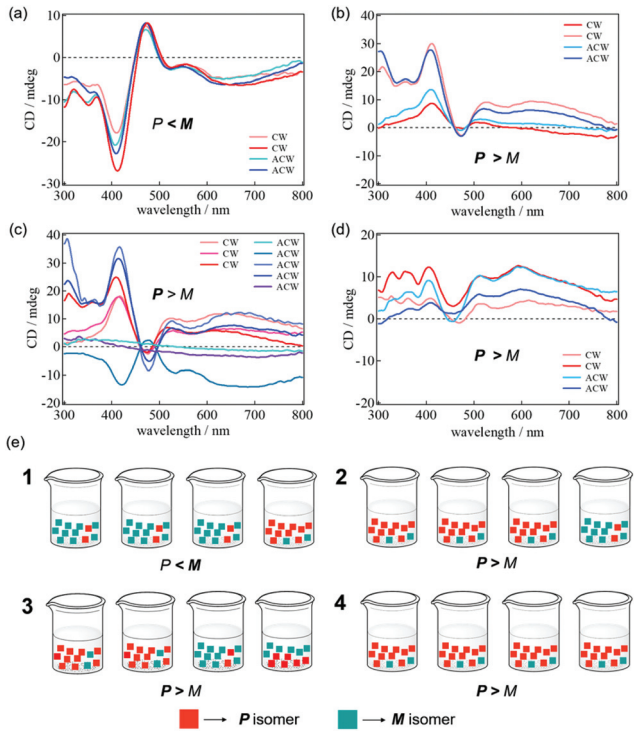

Fig. 3 CD spectra of non-crystalline powder, **1** (a), **2** (b), **3** (c) and **4** (b), obtained by stirring clockwise or anticlockwise. (e) Representation of crystallisation of **1–4**.

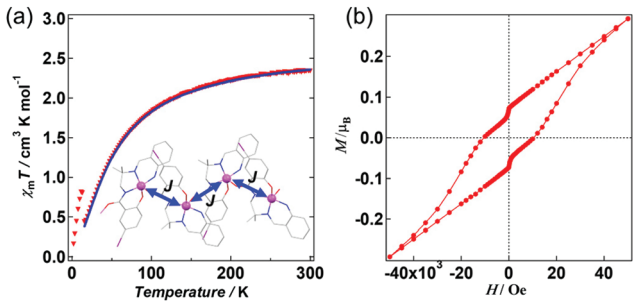

Fig. 4 (a) Temperature dependent magnetic susceptibility of **4**. The solid blue line represents the best fit. (b) *M vs. H* plots at 2.0 K.

not to be exactly isoenergetic and a primary role for PVED in the origin of biomolecular chirality has been suggested.[25] The term 'chiral amnesia'[11] has been applied to the process of rapid racemisation in solution and is considered to be the origin of crystallisation which can produce high enantiomeric excesses in conglomerates of large organic molecules[26] though with random variation in the predominant enantiomorph. The present results imply the operation of more than one of such influences.

In an earlier report, we have shown that compound **1** displayed not only an antiferromagnetic (AF) interaction (J = −2.48 cm^{-1}, g = 1.96) between two Mn(III) ions, but also weak ferromagnetism with a relatively large coercive field of 3.0 kOe at 2 K based on the spin canting of the AF spin ordering.[15] The magnetic susceptibility of complexes **2**, **3**, and **4** was also measured under applied magnetic field (5 kOe) at 2–300 K (Fig. 4 and S11†), giving a RT value for **4** slightly lower than that expected (3.0 cm^3 K mol^{-1}, g = 2) for a high-spin Mn(III) ion (Fig. 4a), with $\chi_m T$ decreasing from 2.33 cm^3 K mol^{-1} at 300 K to 0.438 cm^3 K mol^{-1} at 15.6 K. As the temperature further decreases, $\chi_m T$ steeply increases to a maximum of 0.801 cm^3 K mol^{-1} at 13.1 K, followed by a decrease to 0.15 cm^3 K mol^{-1} at 2 K. The steep increases in $\chi_m T$ at low temperature clearly indicate that a kind of spontaneous magnetization emerges. The experimental data were fitted from 300 to 13 K based on a linear chain and assuming Heisenberg isotropic coupling according to Fisher's expression for S = 2.[27] A molecular field correction was taken into account through the Mean-Field Approximation as zJ' for the interpretation of the magnetic interaction between the chains (see Fig. S11†). The fitted data of **4** give J = −7.77 cm^{-1}, g = 1.88 and zJ' = 0.139 cm^{-1}, and are predicted to include d_{z^2} orbital interactions, as it is assumed to be a major contributor to the magnetic coupling in Jahn–Teller distorted systems.[28] The field dependence of the magnetisation was measured in the range −50 kOe to +50 kOe at 2 K. The magnetisation value reaches *ca.* 0.29$N\beta$ mol^{-1} at 50 kOe, which is far from the expected saturation value of 4.0$N\beta$ mol^{-1} (g = 2 and S = 2). A hysteresis loop in the ordered phase with a remarkably large coercive field of 10 kOe and a remnant magnetisation of 0.075$N\beta$ mol^{-1} were detected in **4**, implying the existence of canted spins (Fig. 4b). The former is more than three times greater than that of compound **1** (3.0 kOe) and, to our knowledge, is the highest of the any species based on Mn(III),[15,29] which decreases with increasing temperature (Fig. S11†). The critical field, estimated as the field at which dM/dH reaches a maximum, is *ca.* 2.5 kOe (Fig. S12†). The magnetisation at various temperatures gradually increases with the field (Fig. S13†), and then increases abruptly, which is indicative of the onset of the field-induced spin-flop transition from the AF phase to a ferromagnetic (F) phase. The M–H curve at above the phase transition temperature (16 K) is completely different from others, indicating the disappearance of the ordered canted spins (Fig. S13†). The canting angle (α) at 2 K was calculated from sin^{-1} (M_w/M_s) and estimated to be ∼2.05°, where M_w is the magnetisation induced by a weak magnetic field and M_s is the saturation magnetisation.[30] The field-cooled magnetisation (FCM) was measured in the field range of 1 to 40 kOe (Fig. S14d†). During the cooling process, a sharp maximum of χ_m at around 14 K under an applied field of 500 and 1000 Oe was observed. This suggests the onset of the AF transition, which may be due to the weak 3D AF ordering in the spin-canted layers. However, the FCM at above 3 kOe shows no maximum and tends to saturate at lower temperatures, indicating that the weak interlayer AF interaction is overcome by the external field to result in an ordered F phase. These features are typically found in field-induced metamagnet. The zero-field-cooled (ZFC) and FCM were measured under an applied field of 5 Oe (Fig. S15d†). Both curves show abrupt increases near 14 K, indicating the occurrence of spin ordering with T_N

= 14 K. The temperature dependence of the *ac* magnetic susceptibilities at different frequencies (Fig. S17c†) exhibits the characteristic peaks with an AF at T_N = 14 K in both in-phase (χ'_m) and the out-of-phase (χ''_m) parts.

The magnetic properties of **2** and **3** were also examined and are shown in Fig. S11 and S14–S17.† The plots for $\chi_m T$ *versus* T indicate that both have AF interactions between Mn(III) ions in the chain with the fitted data as follows: $J = -4.59$ cm^{-1}, g = 1.97, $zJ' = -0.055$ cm^{-1} for **2** and $J = -3.87$ cm^{-1}, g = 1.88, $zJ' = -0.020$ cm^{-1} for **3**. The fitted data of **1–4** indicate that the smaller the $\angle$Mn–O$_{amide}$–C and the shorter the intrachain Mn distances (Table S2†), the stronger the AF interaction between Mn(III) ions. Magnetic hysteresis loops indicate weak ferromagnetism: the coercive fields are 1.4 (**2**) and 0.9 kOe (**3**); the remnant magnetisations are 0.011 (**2**) and 0.009$N\beta$ mol^{-1} (**3**). The canting angles (α) of **2** and **3** are 0.32 and 0.24°, respectively. The temperature of phase transitions (T_N) confirmed by ZFC and FC magnetisation are 8 K for **2** and 7 K for **3**. The temperature dependence of *ac* magnetic susceptibilities of **2** and **3** (Fig. S17†) shows the peak of an AF at each T_N, where the χ'_m reaches a maximum, while no obvious χ''_m was observed. Thus, **2** and **3** may be hidden weak ferromagnets due to spin canting.[29] These detailed investigations show that the magnetism of each compound depends on the separation of Mn(III) ions, both intra- and inter-1D chain, modulated by the halogen substituents so as to control the bulk magnetic properties.

In summary, all the compounds described herein crystallise as unbalanced conglomerates of chiral crystals even though the constituent complexes are all achiral. The chirality of the individual crystals reflects the presence of helical coordination polymer units of one chirality associated with one chirality of the central chelate rings, ***M*** helices being associated with δ conformations or ***P*** with λ in all cases. The chiral environment imposed on the Mn(III) centers renders them dissymmetric, leading to appreciable circular dichroism of the d–d bands in the solid state. Although enantiomeric excesses in the bulk products vary, in all cases there is symmetry breaking in crystallisation of a nature which depends on the ligand substituents. In complex **4** in particular, crystals containing the ***P*** helix of the coordination polymer always appear to predominate. The change of substituents (Cl, Br and I) on the coordinated ligand significantly influences the magnetic properties, with coercive fields of 0.9–10 kOe, that of **4** being the highest known for Mn(III) complexes exhibiting weak ferromagnetism.

Conflicts of interest

There are no conflicts to declare.

Acknowledgements

This work was supported by KAKENHI Grant-in-Aid for Scientific Research (A) JP17H01200.

Notes and references

1 R. M. Hazen, T. R. Filley and G. A. Goodfriend, *Proc. Natl. Acad. Sci. U. S. A.*, 2001, **98**, 5487–5490.
2 (*a*) R. Noyori, *Angew. Chem., Int. Ed.*, 2002, **41**, 2008–2022; (*b*) J.-C. Wang, X. Kan, J.-Y. Shang, H. Qiao and Y.-B. Dong, *J. Am. Chem. Soc.*, 2020, **142**, 16915–16920.
3 J. S. Seo, D. Whang, H. Lee, S. I. Jun, J. Oh, Y. J. Jeon and K. Kim, *Nature*, 2000, **404**, 982–986.
4 D. F. Eaton, *Science*, 1991, **253**, 281–287.
5 X. Zhang, J. Yin and J. Yoon, *Chem. Rev.*, 2014, **114**, 4918–4959.
6 L. Pasteur, *C. R. Acad. Sci.*, 1848, **26**, 535–539.
7 A. Collet, M. J. Brienne and J. Jacques, *Chem. Rev.*, 1980, **80**, 215–230.
8 J. Jacques, A. Collet and S. H. Wilen, *Enantiomers, Racemates, Resolution*, John Wiley & Sons, New York, 1981.
9 T. Ezuhara, K. Endo and Y. Aoyama, *J. Am. Chem. Soc.*, 1999, **121**, 3279–3283.
10 J. Szurgot and M. Szurgot, *Cryst. Res. Technol.*, 1995, **30**, 71–79.
11 C. Viedma, *Phys. Rev. Lett.*, 2005, **94**, 065504.
12 (*a*) A. Maity, M. Gangopadhyay, A. Basu, S. Aute, S. S. Babu and A. Das, *J. Am. Chem. Soc.*, 2016, **138**, 11113–11116; (*b*) I. Bernal and R. A. Lalancette, *C. R. Chim.*, 2015, **18**, 929–934; (*c*) I. Bernal, J. Cai, S. S. Massoud, S. F. Watkins and F. Fronczek, *J. Coord. Chem.*, 1996, **38**, 165; (*d*) I. Bernal, F. Somoza and V. Bahn, *J. Coord. Chem.*, 1997, **42**, 1.
13 S.-W. Cheong and M. Mostovoy, *Nat. Mater.*, 2007, **6**, 13.
14 C. Train, R. Gheorghe, V. Krstic, L.-M. Chamoreau, N. S. Ovanesyan, G. L. J. A. Rikken, M. Gruselle and M. Verdaguer, *Nat. Mater.*, 2008, **7**, 729–734.
15 S. Kusumoto, A. Koga, F. Kobayashi, R. Ohtani, Y. Kim, L. F. Lindoy, S. Hayami and M. Nakamura, *Dalton Trans.*, 2019, **48**, 8617–8622.
16 R. D. Gillard, *The Cotton Effect in Coordination Compounds, in Progress in Inorganic Chemistry*, ed. F. A. Cotton, John Wiley & Sons, Inc., USA, 1967, vol. 7.
17 I. Bernal, *J. Chem. Educ.*, 1992, **69**, 468.
18 M. Matsushima, K. Wada, Y. Horino, K. Takahara, Y. Sunatsuki and T. Suzuki, *CrystEngComm*, 2020, **22**, 458–466.
19 C. Viedma, *Cryst. Growth Des.*, 2007, **7**, 553–556.
20 V. Marichez, A. Tassoni, R. P. Cameron, S. M. Barnett, R. Eichhorn, C. Genet and T. M. Hermans, *Soft Matter*, 2019, **15**, 4593–4608.
21 K. Suwannasang, A. E. Flood, C. Rougeot and G. Coquerel, *Cryst. Growth Des.*, 2013, **13**, 3498–3504.
22 D. K. Kondepudi, J. Laudadio and K. Asakura, *J. Am. Chem. Soc.*, 1999, **121**, 1448–1451.
23 (*a*) W. Meyerhoffer, *Chem. Ber.*, 1904, **37**, 2604–2610; (*b*) C. Viedma, B. J. V. Verkuijl, J. E. Ortiz, T. d. Torres, R. M. Kellogg and D. G. Blackmond, *Chem. – Eur. J.*, 2010, **16**, 4932–4937.

24 C. Tschierske and G. Ungar, *ChemPhysChem*, 2016, **17**, 9–26.
25 A. Szabó-Nagy and L. Keszthelyi, *Proc. Natl. Acad. Sci. U. S. A.*, 1999, **96**, 4252–4255.
26 D. G. Blackmond, *Chem. – Eur. J.*, 2007, **13**, 3290–3295.
27 M. E. Fisher, *Am. J. Phys.*, 1964, **32**, 343.
28 J. H. Yoon, D. W. Ryu, H. C. Kim, S. W. Yoon, B. J. Suh and C. S. Hong, *Chem. – Eur. J.*, 2009, **15**, 3661–3665.
29 (*a*) D.-F. Weng, Z.-M. Wang and S. Gao, *Chem. Soc. Rev.*, 2011, **40**, 3157–3181; (*b*) K.-L. Hu, M. Kurmoo, Z. Wang and S. Gao, *Chem. – Eur. J.*, 2009, **15**, 12050–12064.
30 O. Kahn, *Molecular Magnetism*, VCH, Weinheim, Germany, 1993.